CHAPTER IV
RESULTS AND DISCUSSION

4.1 Characterization of Synthesized Products

The synthesized products of tetra-coordinated spirosilicates, C2 and aminospirosilicate, C4 were prepared following Sun's work. The synthesized products were identified using FTIR, NMR and TGA, as described following.

4.1.1 Fourier Transform Infrared (FTIR) Spectroscopy

The white powder products of tetra-coordinated spirosilicates, C2 and aminospirosilicate, C4 were characterized by mixing with KBr, as shown in figure 4.1. The characteristic peaks of each product are summarized in table 4.1

Table 4.1 The FTIR bands of C2 and C4.

Products	Functional groups	Wave number (cm^{-1})
Monomer :C2	O-H stretching C-H stretching Si-O-CH stretching (Sun,2000)	Broad band at 3405 cm^{-1} 2951-2883 cm^{-1} 1086, 944, and 883 cm^{-1}
Monomer :C4	O-H stretching C-H stretching Si-O-CH stretching (Sun,2000)	Broad band at 3405 cm^{-1} 2951-2883 cm^{-1} 1086 and 944 cm^{-1}

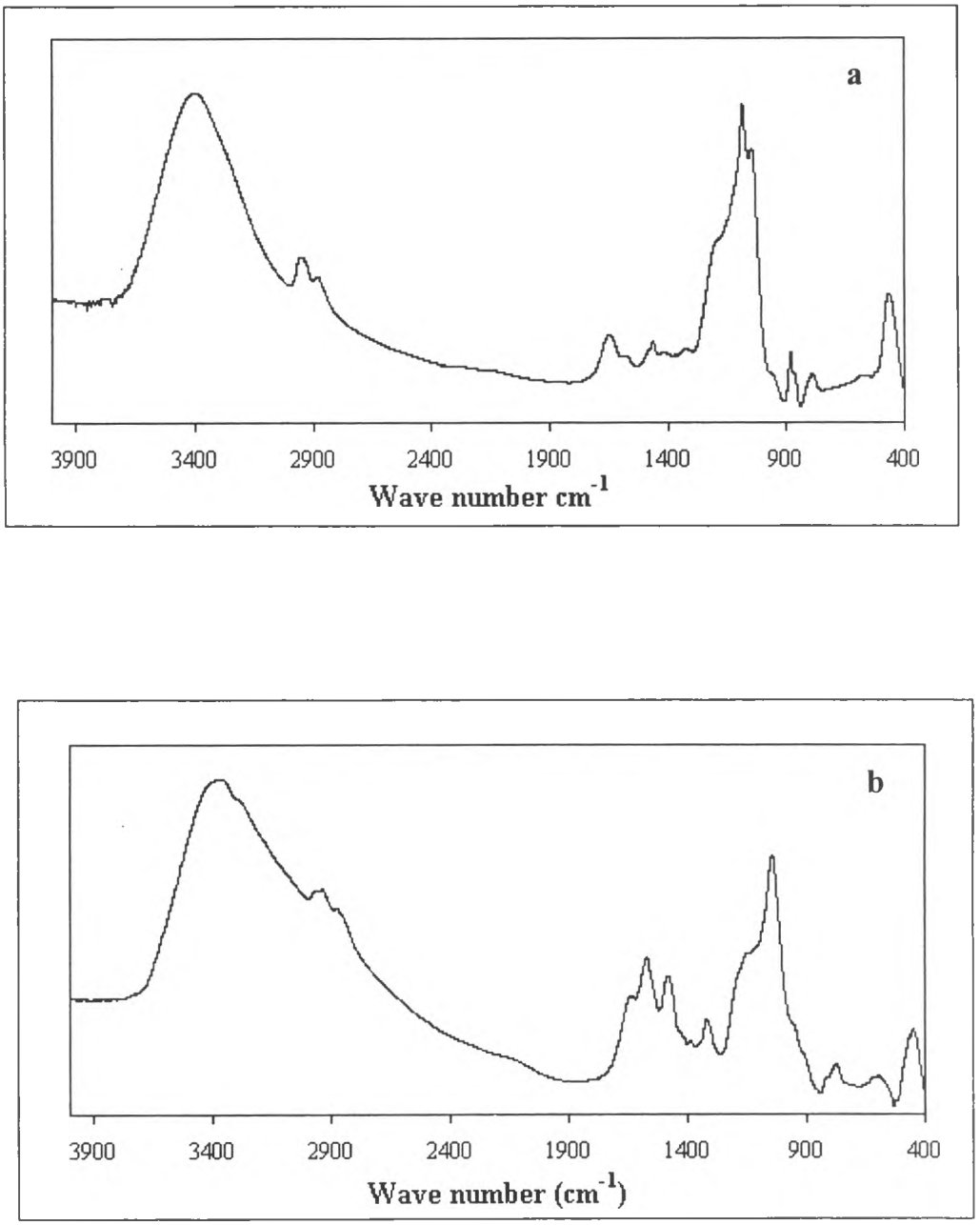

Figure 4.1 FTIR spectra of tetra-coordinated spirosilicates, a) C2 and b) amino, C4.

4.1.2 Proton and Carbon Nuclear Magnetic Resonance Spectroscopy (^{1}H- and ^{13}C-NMR)

The spectra of ^{1}H- and ^{13}C-NMR of tetra-coordinated spirosilicates, C2 and amino C4, are shown in figures 4.2 and 4.3, respectively. The results are summarized in table 4.2.

Table 4.2 The ^{1}H- and ^{13}C-NMR spectra of spirosilicate species.

Type of products	Chemical shift (ppm)		Assignment
	^{1}H-NMR	**^{13}C-NMR**	
Monomer :C2	3.27	62.75	CH_2-O
Monomer :C4	0.83	22.11	CH_3
	-	53.47	C
	3.13	67.12	CH_2-O

4.1.3 Thermogravimetric Analysis (TGA)

The result of TGA, as indicated in figure 4.4 gave the final ceramic yields for monomers C2 and C4 42.74%, and 34.16%, respectively. The theoretical yields of both are 40.05% and 25.64%, respectively. The differences are due to the further crosslinking of the monomers during heating since the final residue was black.

FTIR, NMR and TGA results indicated that the spirosilicates were successfully synthesized.

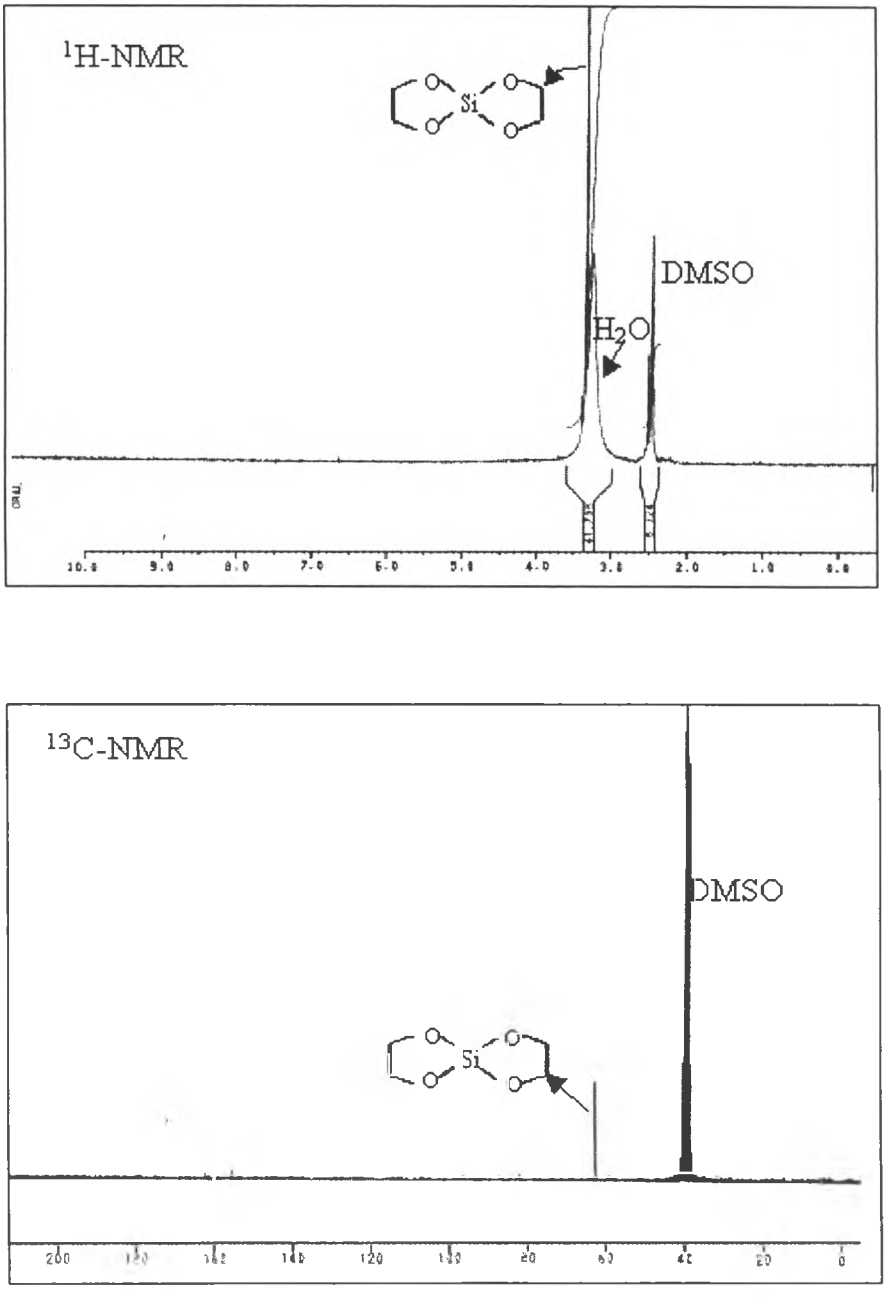

Figure 4.2 ^{1}H-and ^{13}C-NMR spectra of tetra-coordinated spirosilicate, C2.

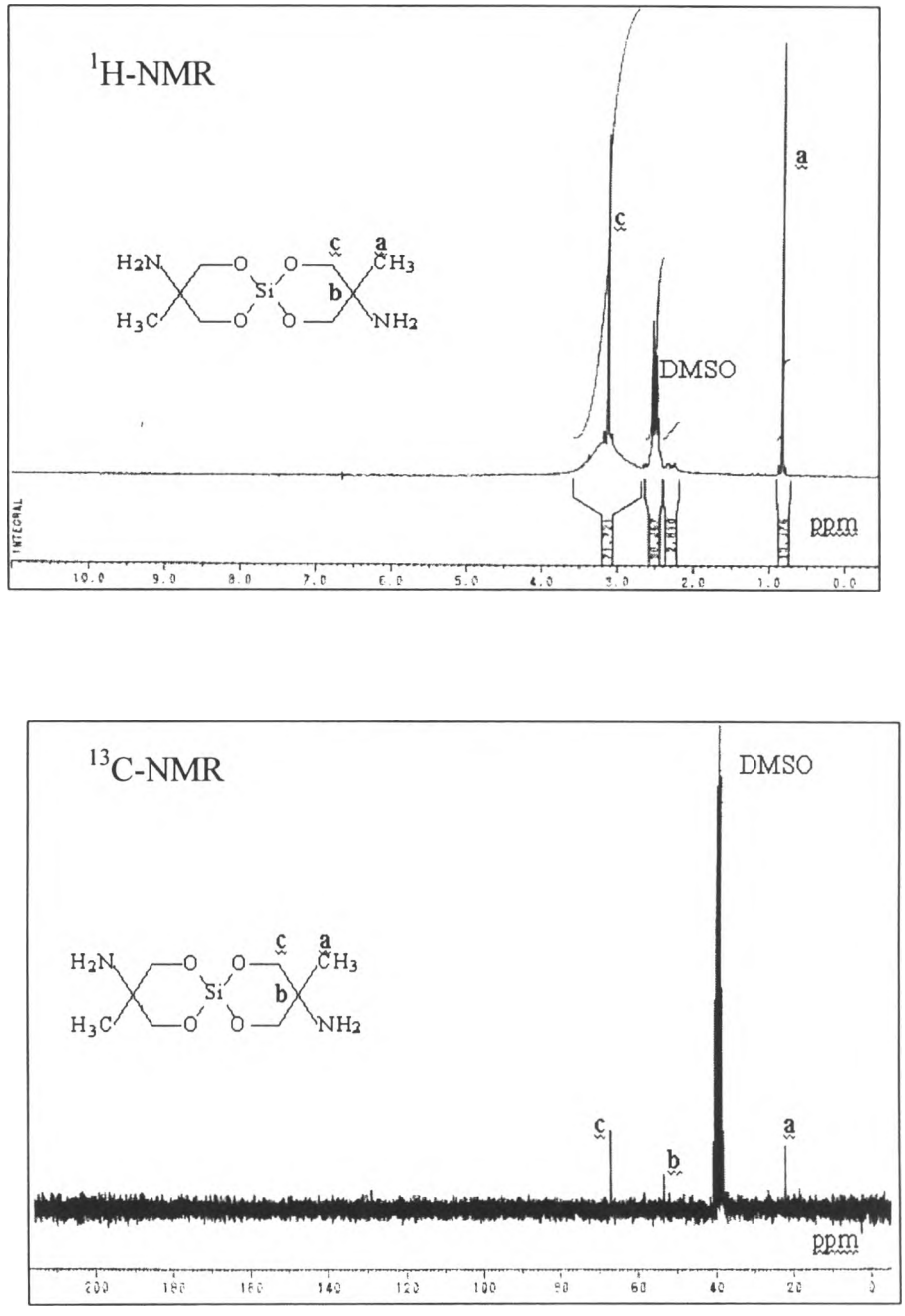

Figure 4.3 ^{1}H-and ^{13}C-NMR spectra of aminospirosilicate, C4.

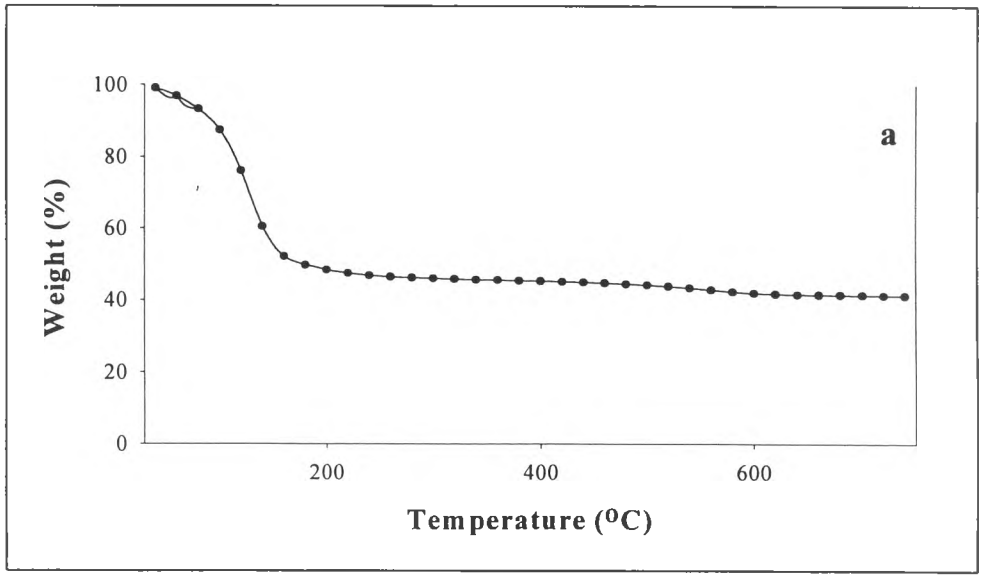

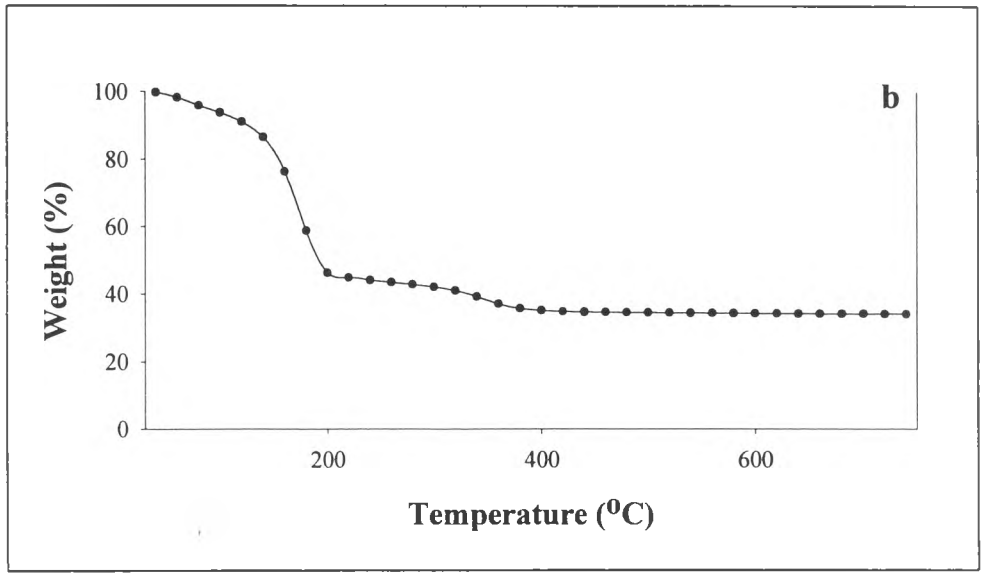

Figure 4.4 TGA thermograms showing (%) weight loss due to thermal changes of tetra-coordinated a) spirosilicate, C2 and b) aminospirosilicate, C4.

4.2 Study of Curing Conditions

4.2.1 Polymer C2

The synthesized products of C2 polymer, was first conducted by studying the variations of reaction temperature and time, as shown in table 4.3.

Table 4.3 Effect of temperature and time on the synthesis of C2 polymer.

Temperature (°C)	**Ceramic Yield (%)**	
	3 h	**5 h**
110	42.50	45.40
120	49.28	50.55
130	50.90 Difficult to purify	Too viscous to purify

From table 4.3 the C2 polymer product was cured by first varying temperature and fixing the time at 3 h. The ceramic yield approached a constant value at 120°C. The curing time studied was continued to 5 h with the same range of temperature. As a result, it was found that the curing condition at 120°C for 5 h gave ceramic yields comparable to those for 3 h. Therefore, the synthesized product at 120°C for 3 h was chosen as the optimum ceramic yield to get high crosslink product.

The synthesized product of polymer C2 was identified using FTIR, NMR and TGA, as described following

4.2.1.1 Fourier Transform Infrared (FTIR) Spectroscopy

The white product of C2 polymer was characterized by mixing with KBr, as shown in table 4.4 and figure 4.5. The O-H stretching was due to the water absorbed in the product.

Table 4.4 The assignments of FTIR bands of polymer C2.

Products	**Functional groups**	**Wave number (cm^{-1})**
Polymer :C2	O-H stretching	Broad band at 3405 cm^{-1}
	C-H stretching	2951-2883 cm^{-1}
	Si-O-CH stretching	1086, 944, and 883 cm^{-1}

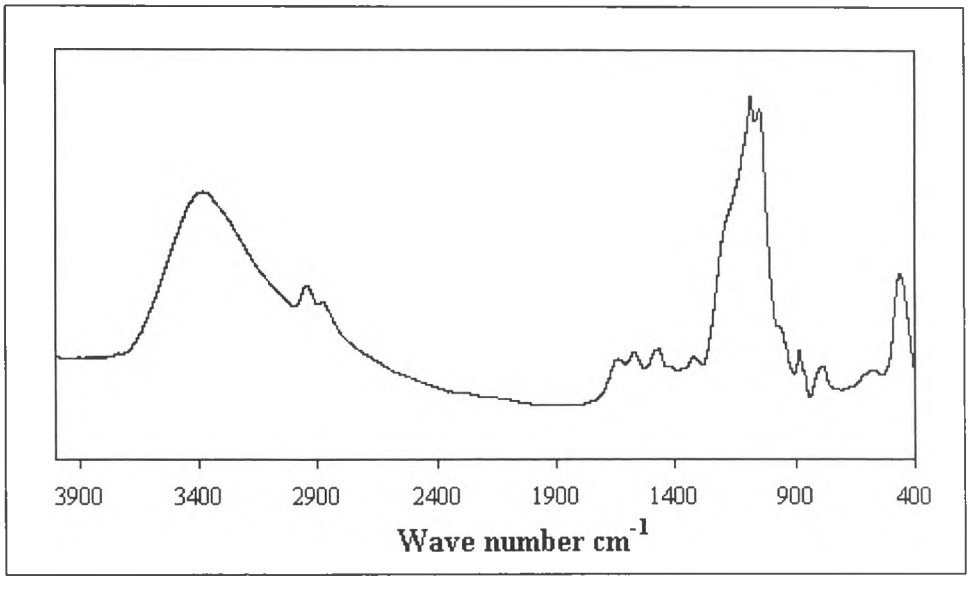

Figure 4.5 FTIR spectrum of C2 polymer.

4.2.1.2_Proton and Carbon Nuclear Magnetic Resonance Spectroscopy (^{1}H- and ^{13}C-NMR)

The spectra of ^{1}H- and ^{13}C-NMR of C2 polymer are summarized in table 4.5 and shown in figure 4.6. The spectrum positions are the same as those of C2 monomer.

Table 4.5 The spectrum assignments of ^{1}H- and ^{13}C-NMR of spirosilicates C2.

Type of products	Chemical shift (ppm)		Assignment
	^{1}H-NMR	^{13}C-NMR	
Polymer :C2	3.27	62.75	$\underline{CH_2}$-O

4.2.1.3 Thermogravimetric Analysis (TGA)

The result of TGA, as indicated in figure 4.7-a, gave the final ceramic yield for polymer C2 as 49.28% due to the crosslinking of glycolato silicate monomer, leading to highly branched materials (Crandall, 1995), as compared to C2 monomer. The results are readily confirmed by comparison of both decomposition temperatures, as shown in figure 4.7, thus we observe a shift of the decomposition point of monomer, 114.97°C, toward a higher temperature, 126.33°C, for polymer.

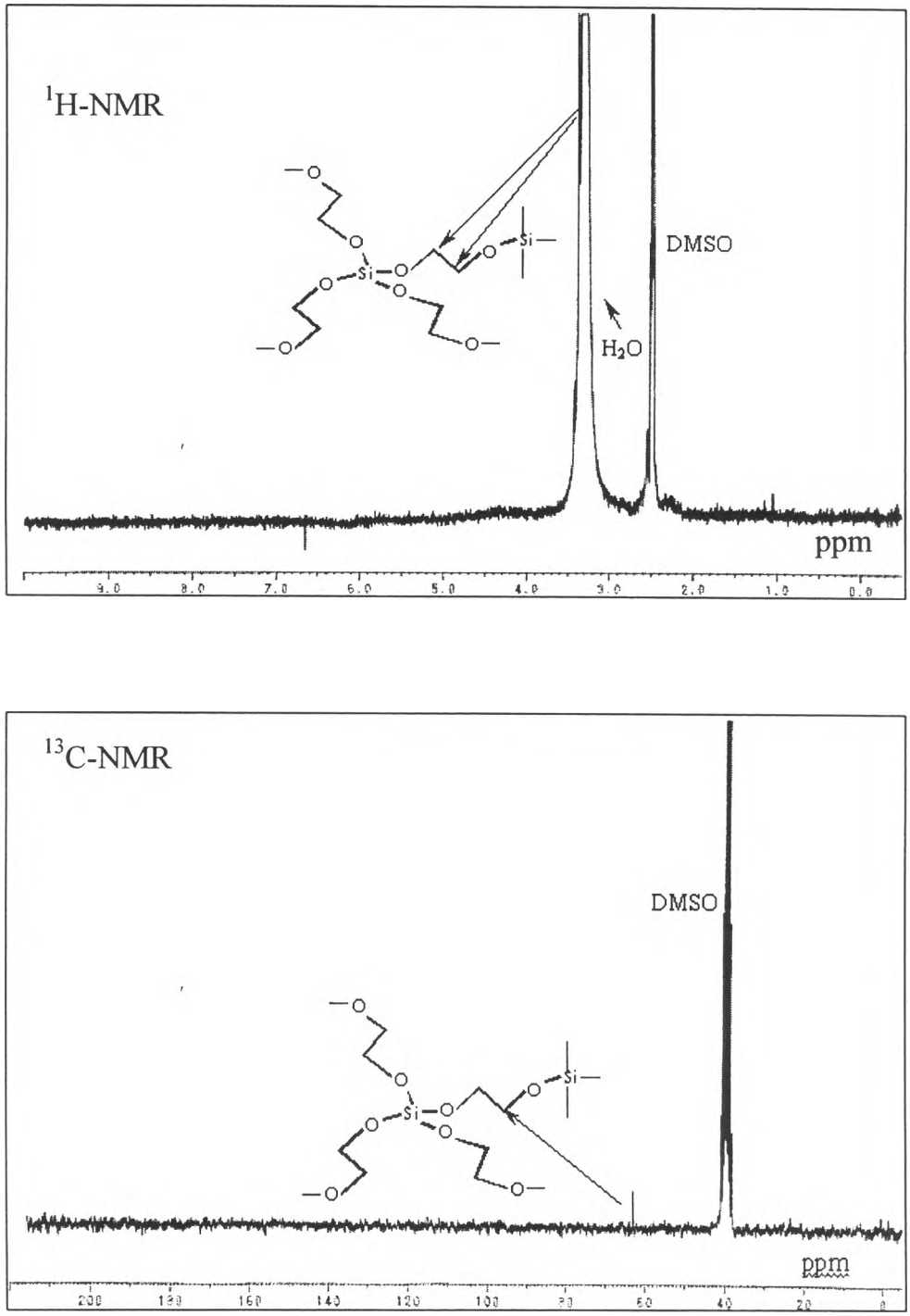

Figure 4.6 ^{1}H-and ^{13}C-NMR spectra of C2 polymer.

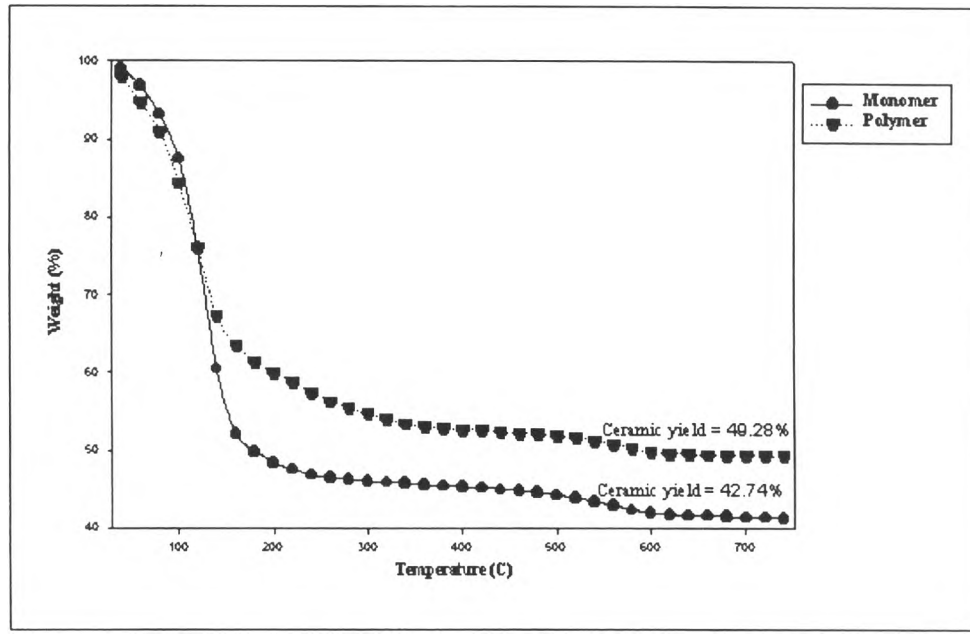

Figure 4.7-a TGA thermograms showing (%) weight loss due to thermal changes.

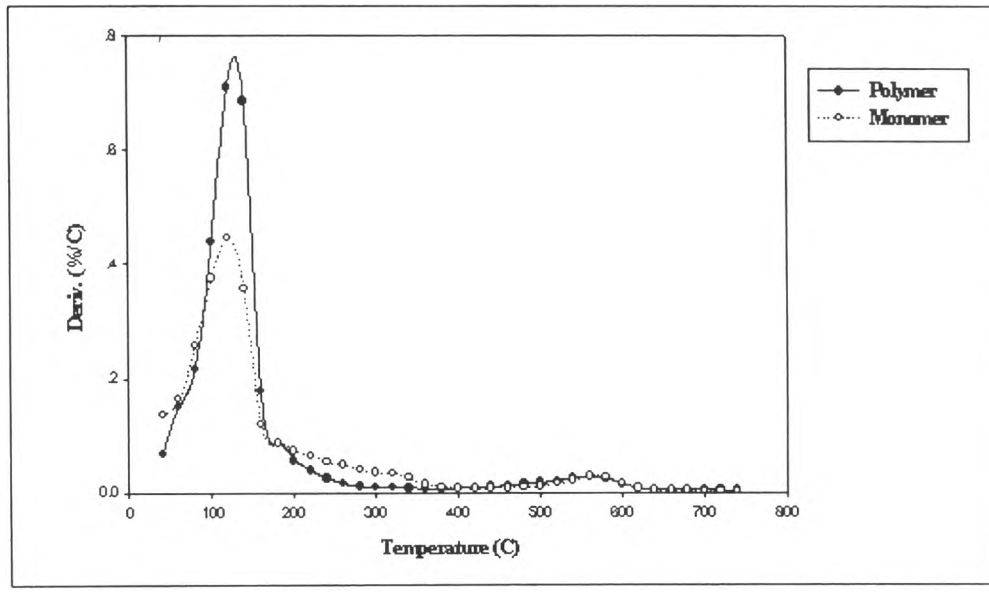

Figure 4.7-b TGA thermograms showing decomposition temperatures of C2 monomer and polymers.

4.2.2 Polymer C4

Similarly, the optimum curing condition of C4 polymer product was carried out in the same manner. The curing condition was studied by varying temperature and time, as shown in table 4.6.

Table 4.6 Effect of temperature and time on the synthesis of C4 polymer.

Temperature (°C)	**Ceramic Yield (%)**	
	5 h	**10 h**
170	46.71	45.37
180	46.36	45.99

It was found that the resulting in the highest ceramic yields obtained was at 170°C for 5 h, as reported in table 4.6.

The synthesized product of C4 polymer was identified using FTIR, NMR and TGA, as described following

4.2.2.1 Fourier Transform Infrared (FTIR) Spectroscopy

The white product of C4 polymer was characterized by mixing with KBr, as shown in table 4.7 and figure 4.8. The O-H stretching was due to the water absorbed in the product.

Table 4.7 The assignments of FTIR bands of C4 polymer.

Products	Functional groups	Wave number (cm^{-1})
Polymer :C4	O-H stretching	Broad band at 3405 cm^{-1}
	C-H stretching	2951-2883 cm^{-1}
	Si-O-CH stretching	1086 and 944 cm^{-1}

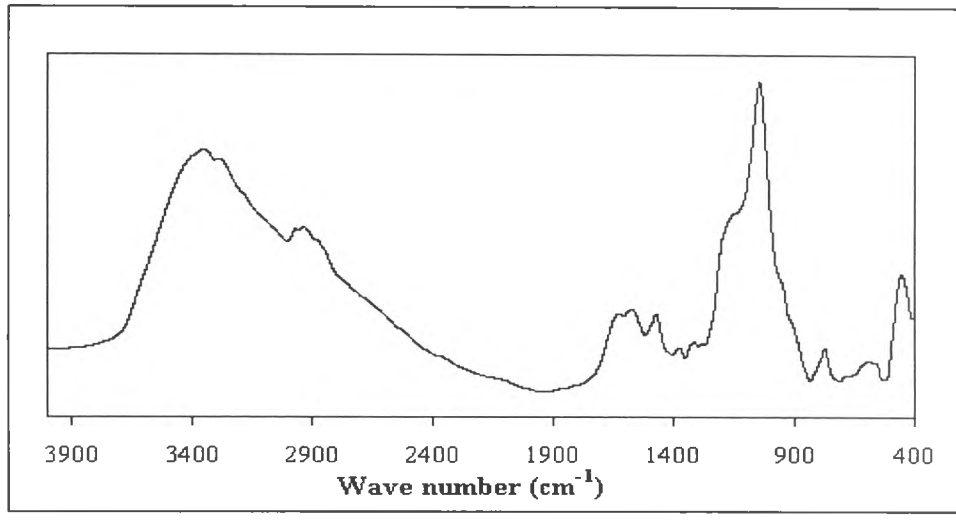

Figure 4.8 FTIR spectrum of polymer C4.

4.2.2.2 Proton and Carbon Nuclear Magnetic Resonance Spectroscopy (^{1}H- and ^{13}C-NMR)

The spectra of ^{1}H- and ^{13}C-NMR of C4 polymer are summarized in table 4.8 and shown in figure 4.9. The spectrum positions are the same as those of C4 monomer.

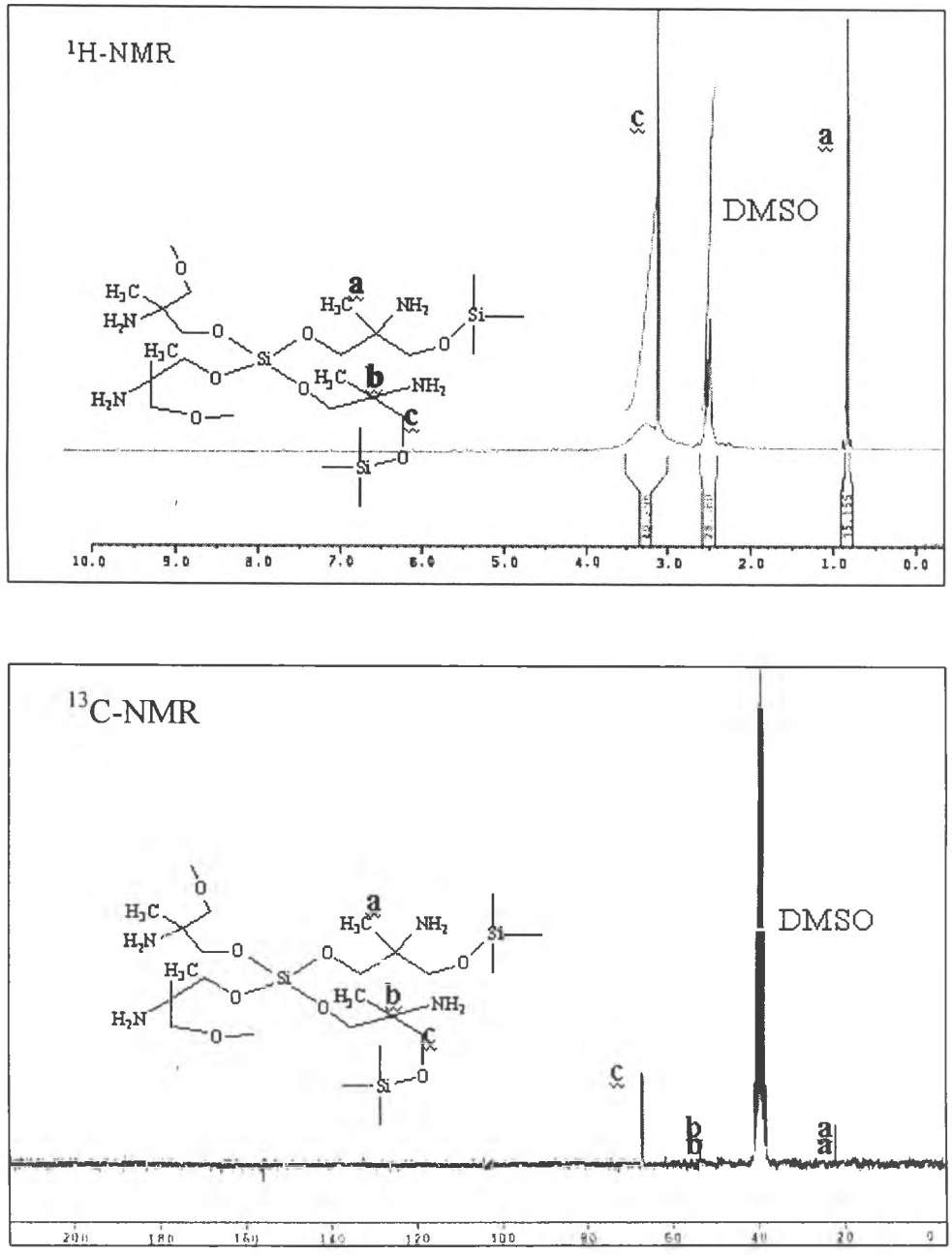

Figure 4.9 ^{1}H-and ^{13}C-NMR spectra of C4 polymer.

Table 4.8 The spectrum assignments of ^{1}H- and ^{13}C-NMR of aminospirosilicate C4.

Type of products	Chemical shift (ppm)		Assignment
	^{1}H-NMR	^{13}C-NMR	
Polymer :C4	0.83	22.11	$\underline{CH_3}$
	-	53.47	$\underline{C}$
	3.13	67.12	$\underline{CH_2}$-O

4.2.1.3 Thermogravimetric Analysis (TGA)

The result of TGA, as indicated in figure 4.10, gave the final ceramic yield for polymer C4 was 46.71% due to the crosslinking, leading to highly branched materials (Crandall, 1995), as compared to C4 monomer.

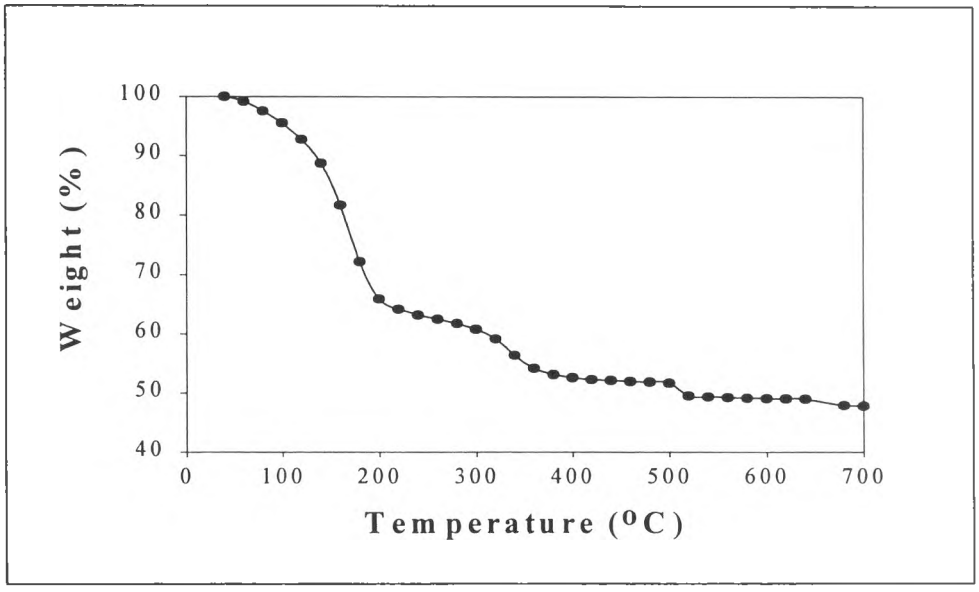

Figure 4.10 TGA thermogram showing (%) weight loss due to thermal changes.

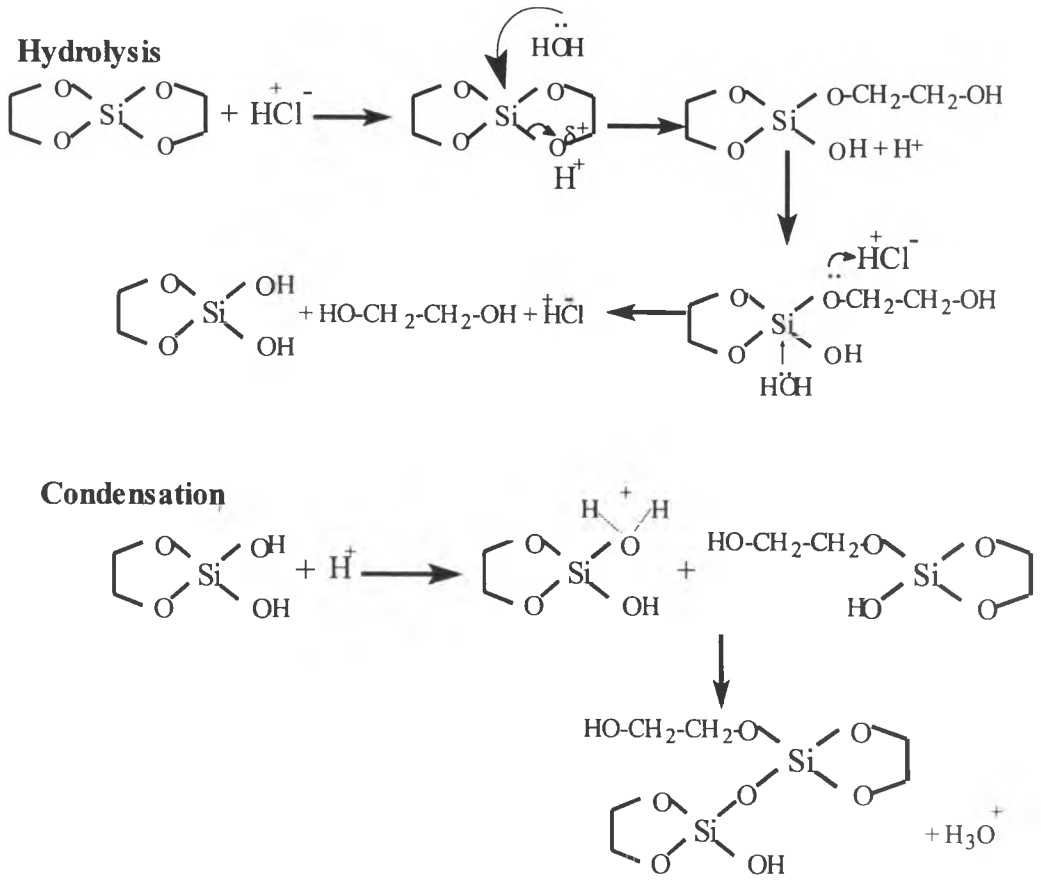

Figure 4.11 Schematic of hydrolysis and condensation under hydrochloric acid solution.

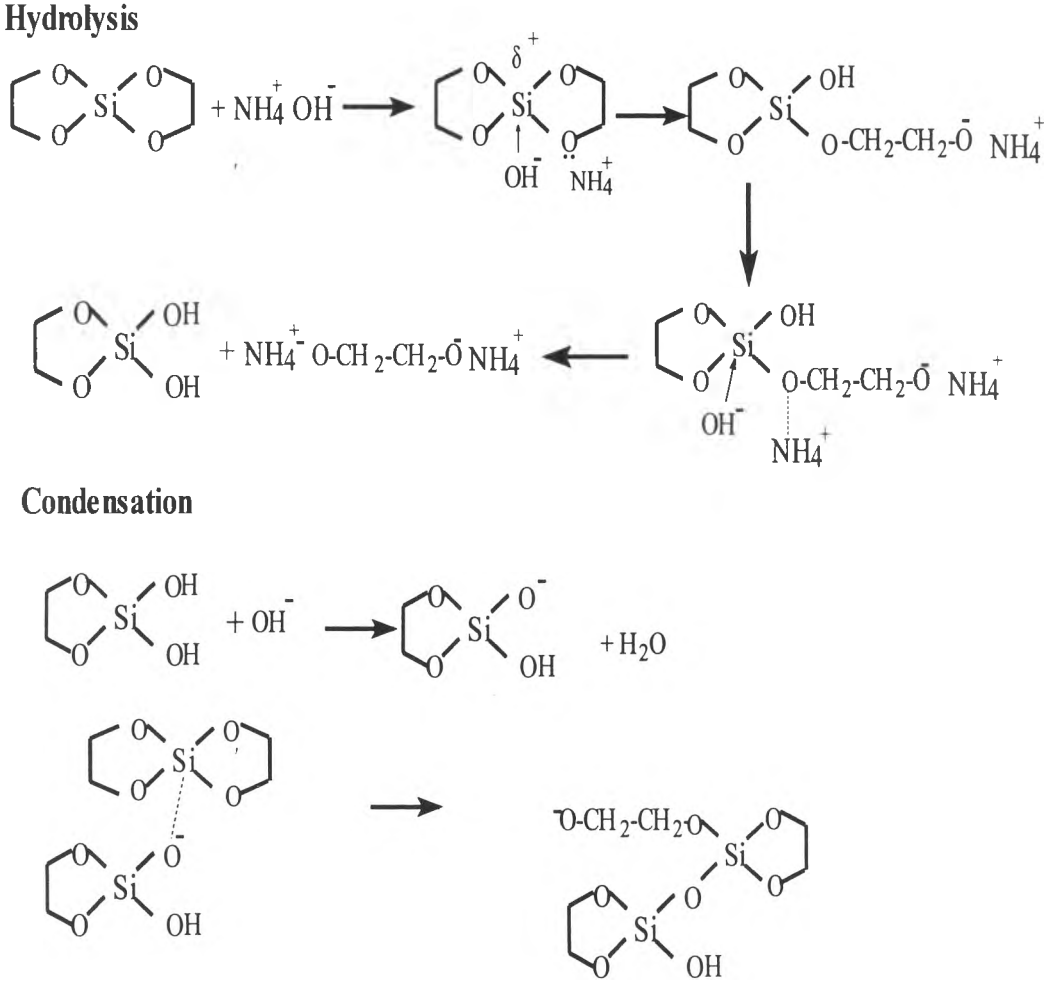

Figure 4.12 The schematic of hydrolysis and condensation under ammonium hydroxide solution.

4.3 Sol-gel transition study

It is the well known that the catalyst used in a gelation reaction can have large effects on the microstructure of the gels formed as well as on the rapidity of the gelation process (Mackenzie, 1986). During sol to gel transition induced by applying solvent, the polymerization occurs via hydrolysis and polycondensation reaction. Figures 4.11 and 4.12 show two proposed mechanisms of hydrolysis and condensation for tetracoordinated spirosilicates under acidic and base conditions.

The hydrolyzed products of monomer C2 were identified using FTIR and TGA, as described below.

4.3.1 Fourier Transform Infrared (FTIR) Spectroscopy

4.3.1.1 Using 1M hydrochloric acid solution

From figure 4.13 (a) using 1% of 1M HCl, it was shown that the characteristic peaks at 3405, 2951, 2883, 1086 and 883 cm^{-1} decreased as the time increased. The decrease in the absorption at 3405 cm^{-1} was attributed to the decrease in the amount of Si-OH due to the condensation of silanols (Yamane, 1988). At the same time, the absorption peak around 1648 cm^{-1}, which was assigned to the OH bending (Jung, 2000), also decreased in the same manner. The change in the absorption peak at 1086 cm^{-1} suggests that crosslinking of Si-O-Si bonds occurs via hydrolysis and condensation. This was confirmed by comparison with the disappearance of absorption peaks at 3405, 2951, 2883 cm^{-1}, indicating a decrease of organic groups (carbon atom). It should be noted that at 9 h the absorption peaks at 3405, 2951, 2883, 1086 and 883 cm^{-1} were changed in reverse direction (Brinker, 1988, 1990), and further decreased again at 10 h and obtained the final result at 11 h.

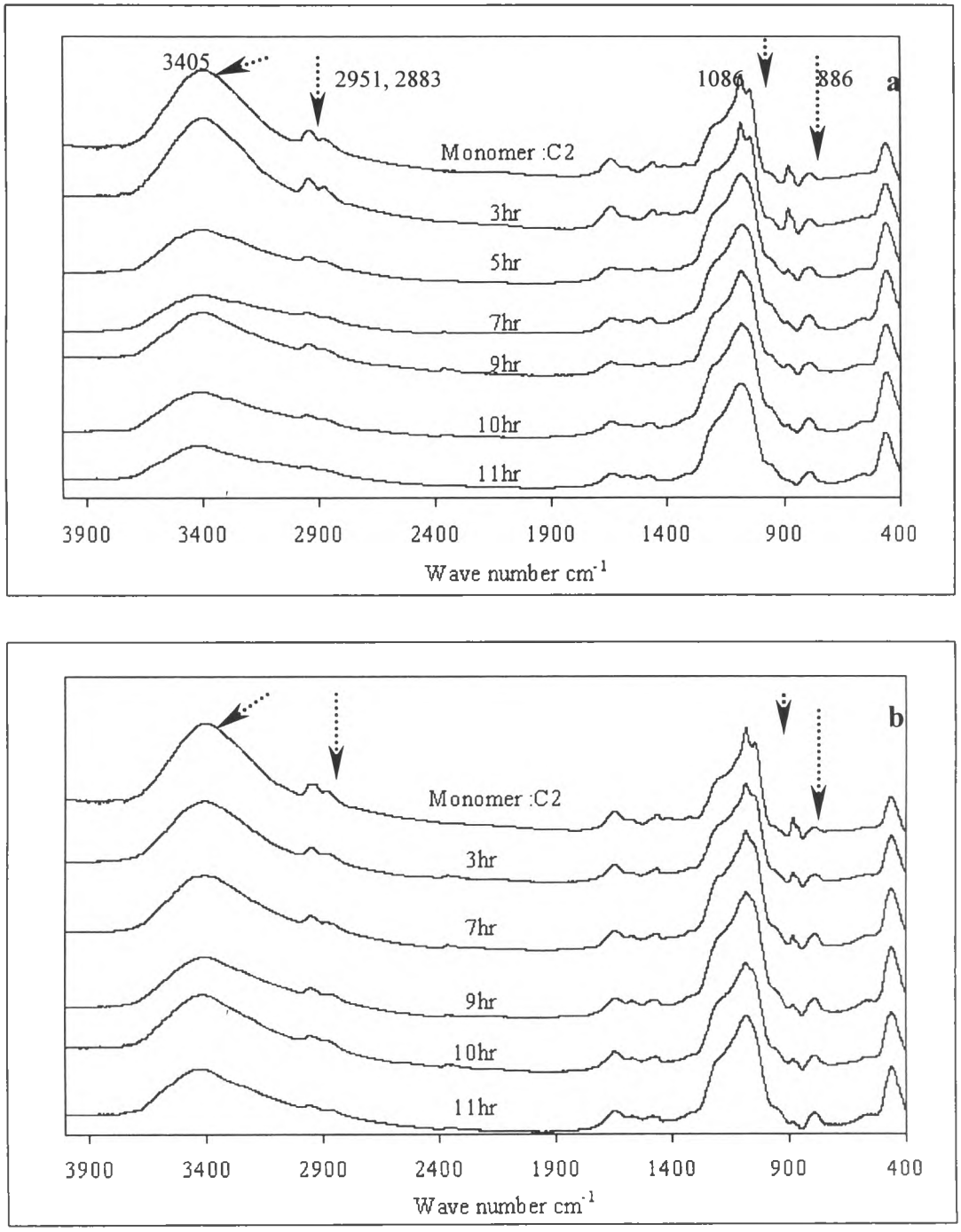

Figure 4.13 FTIR spectra of hydrolyzed C2 monomer product with (a) 1% and (b) 2% of 1M HCl at room temperature.

The structure at this point of hydrolyzed product obtained was very close to that of silica. The FTIR structure of fused silica is shown in figure 4.14.

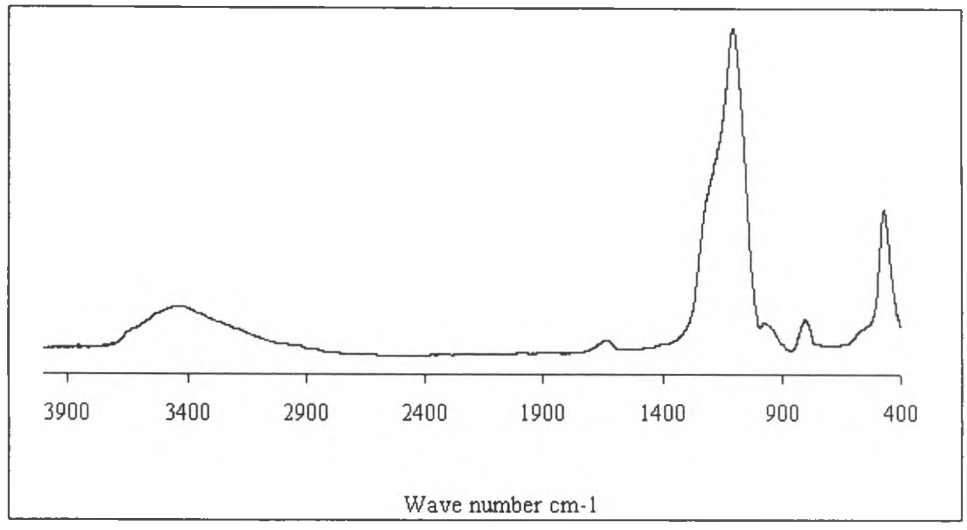

Figure 4.14 FTIR spectrum of fused silica.

From figure 4.13 (b) for 2% of 1M HCl, the obtained results were almost the same as figure 4.13 (a). In addition, the change of absorption peaks at 3405, 2951, 2883, 1086 and 886 cm^{-1} initially decreased faster in the beginning when compared to lower concentration of HCl used.

The results are shown more clearly in the figure 4.15, which displays the relationship between the ratio of Si-O-CH stretch/ Si-O (the absorption peak at 1086 cm^{-1} and 463 cm^{-1}, internal reference peak) plotted against time for hydrolysis of the C2 monomer at various acid concentrations at room temperature.

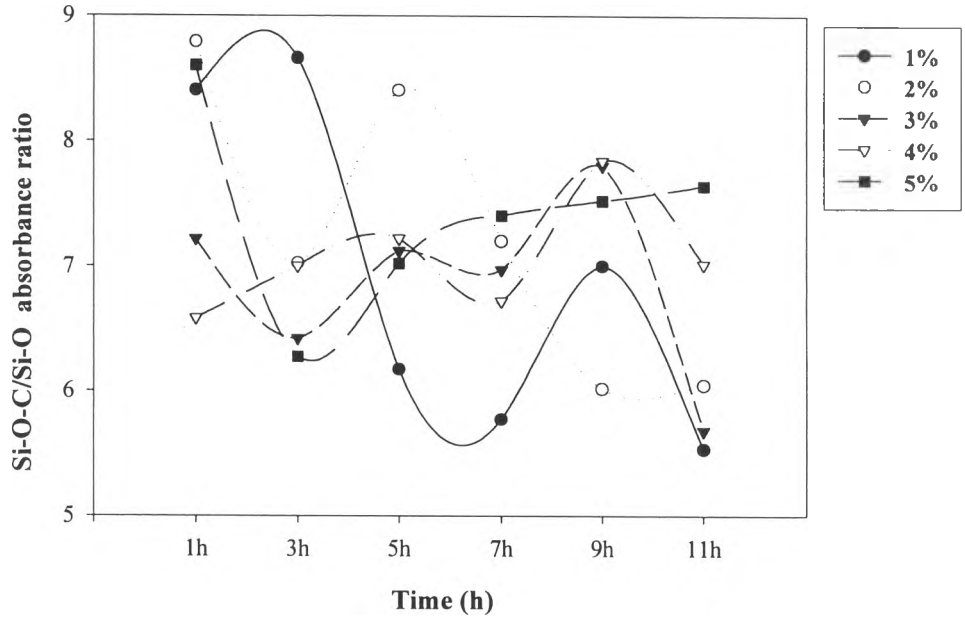

Figure 4.15 The time-dependence of hydrolyzed products of C2 monomer with 1%-5% of 1M HCl at room temperature.

The results indicate that the optimum condition, showing a good trend of hydrolysis sequence, is when the 1% of 1M HCl is applied, as studied by Lippert in 1988 for TEOS. Thus, this condition again was selected to apply for studying the effect of temperature, as can be seen in figure 4.16. It was found that at 40°C the rate of decrease of absorption peaks at 3405, 2951, 2883, 1086 and 883 cm^{-1} was much faster than at room temperature.

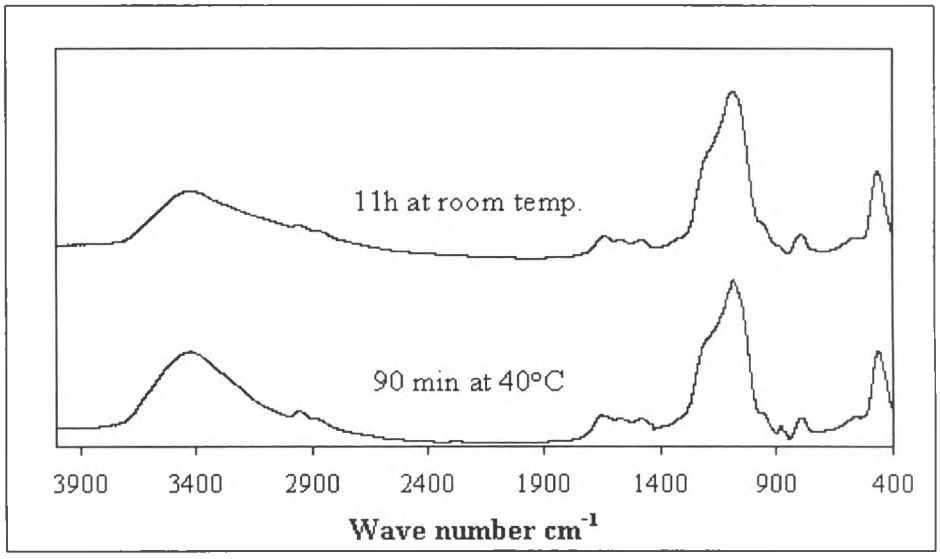

Figure 4.16 FTIR spectra showing the effect of temperature on the hydrolyzed product.

4.3.1.2 Using 1M ammonium hydroxide solution

Figure 4.17 shown dependence of the ratio of Si-O-C/Si-O-Si absorption peaks versus hydrolysis time for different concentration of NH_4OH. From figure 4.17, for 1% of 1M NH_4OH, the results of the structural change from Si-O-C to Si-O-Si show little bit change, compared to that between monomer and hydrolyzed product, in the time period from 1 h to 8 h. After 9 h, a substantial decrease of the peak ratio was observed. Subsequently, however, after 11 h, the ratio increased again.

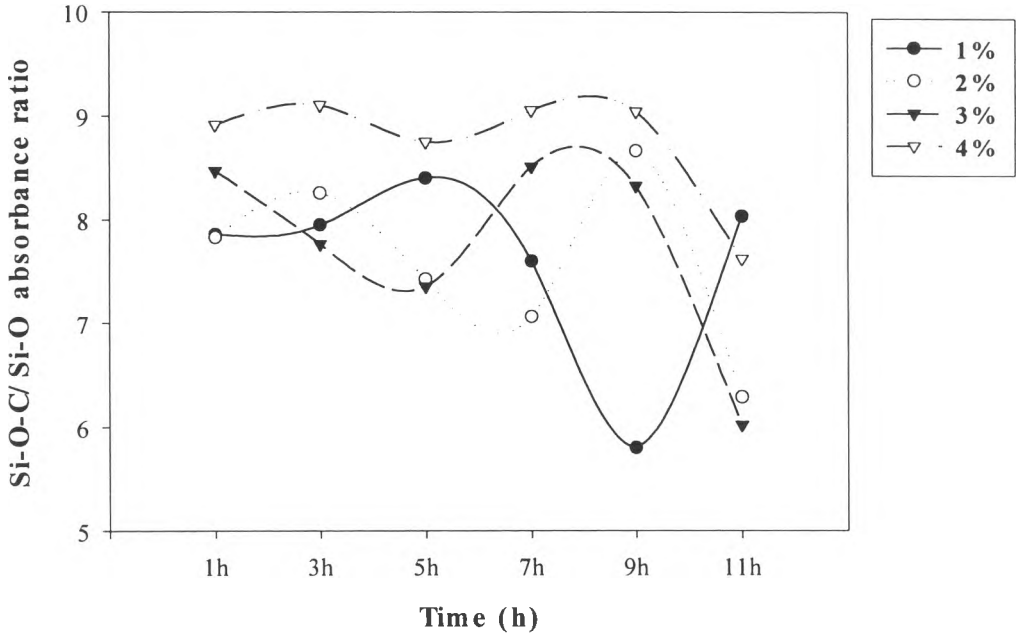

Figure 4.17 The time-dependence of hydrolyzed products of monomer C2 with 1%-4% of 1M NH_4OH at room temperature.

In summary, the kinetics of the sol-gel transition of C2 monomer are slowest at 1% and 2% of 1 M HCl, due to the absence of ionized hydroxyl groups [Si-O^- or Si-$(OH_2)^+$] (LaCourse 1988), for which pH ≈ 2, as monitored by decrease of absorption peaks at 3405, 2951, 2883, 1086 and 883 cm^{-1}, consistent with experimental studies of Brinker and coworkers (Brinker, 1990), who determined the optimal gel time of TEOS to be at pH near 2.

Table 4.9 The pH results of different catalyst concentration.

Concentration of HCl (1M)	**pH result**	**Concentration of NH_4OH (1M)**	**pH result**
1%	2.14	1%	9.56
2%	2.03	2%	9.67
3%	1.97	3%	9.72
4%	1.81	4%	9.80
5%	1.73	5%	10.1
15%	0.65	15%	10.2

4.3.2 Thermogravimetric Analysis (TGA)

The TGA results of monomer after hydrolysis with 1% and 2% of 1M HCl were chosen to study due to the slow polymerization, as shown in figures 4.13 and 4.15. Those showed significant of decrease in the absorption peaks at 3405, 2951, 2883, 1086 and 883 cm^{-1}. The ceramic yields of the product obtained from both conditions are shown in figure 4.18 (a) and (b) and in table 4.10.

Table 4.10 The ceramic yields of the hydrolyzed monomer after using 1M HCl at various gelation time.

Time (h)	Ceramic Yield (%)	
	1% of 1M HCl	2% of 1M HCl
3	44.34	51.92
5	58.61	46.11
7	62.68	56.21
9	57.13	63.02
10	64.86	-
11	66.29	64.88

Evidently, the kinetic data obtained from FTIR spectra and the ceramic yields from TGA are in agreement. A decrease in the absorption peaks of Si-O-C and increase in Si-O-Si peaks correlates to an increase of ceramic yield. Notably, as the increase of Si-O-C peaks at 9 h compared to 7 and 10 h at 1% of 1M HCl, agrees with a decrease of ceramic yield from TGA.

Those results suggest surprisingly that the reaction can be proceed in the reverse direction, so called "reesterification", in which an alcohol molecule displaces a hydroxyl group to produce an alkoxide ligand and water as a by product (Brinker 1984, 1990).

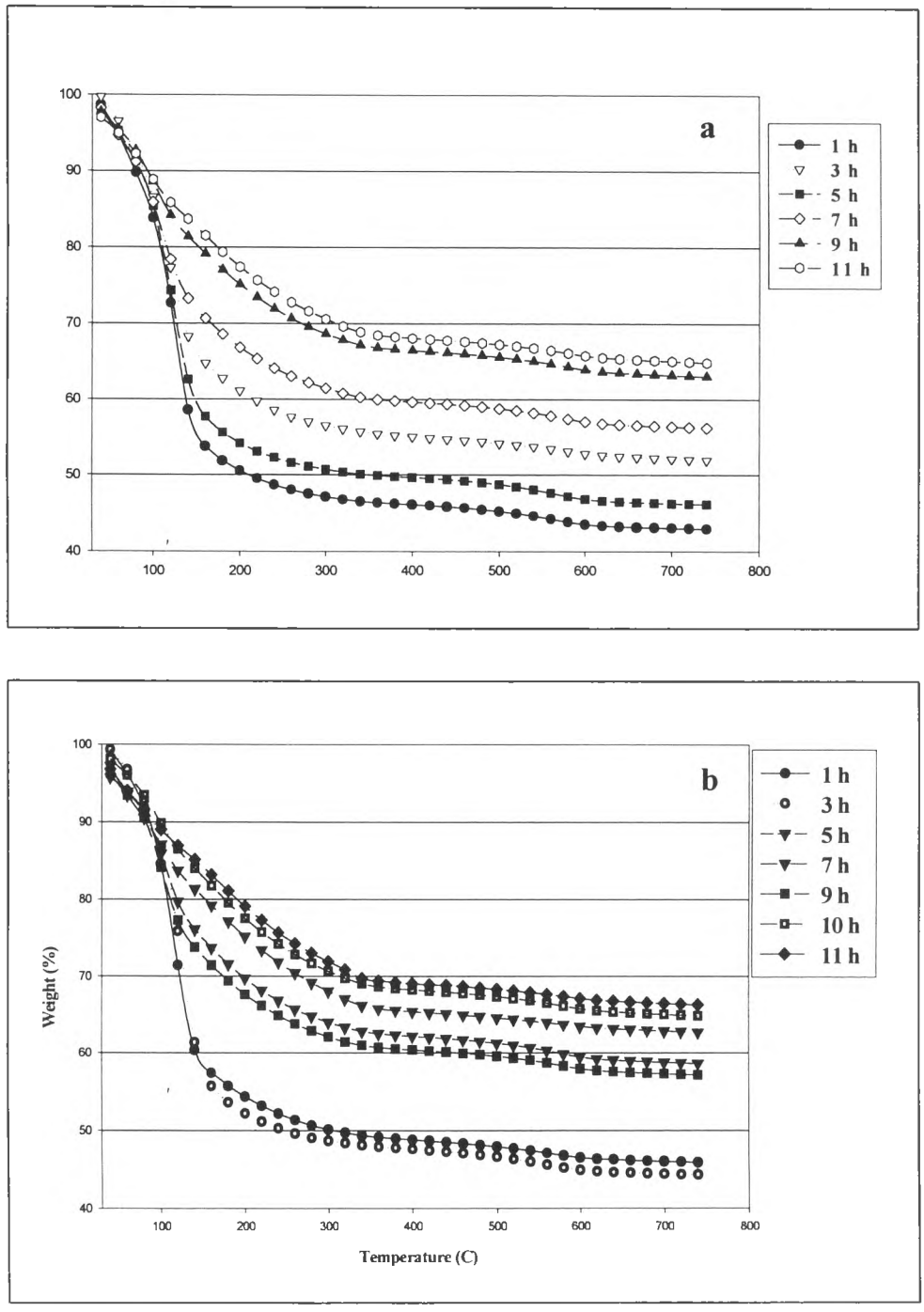

Figure 4.18 TGA thermograms showing percent ceramic yield at various times after hydrolysis with 1M HCl at (a) 1% and (b) 2%.

4.4 Characterization of Pyrolyzed C2 Monomer

4.4.1 BET Surface Area Measurement

The BET surface area study of pyrolyzed product obtained from 4.3.1.1 at 750°C for 7 h is shown in table 4.11.

Table 4.11 The BET surface area measurement of monomer after hydrolysis with 1% of 1M HCl and NH_4OH at various times, followed by pyrolysis at 750°C for 7 h, is compared to fused-silica (starting material).

Time (hr.)	Surface area (m^2/g)	
	1% of 1M HCl	1% of 1M NH_4OH
3	307	296
5	354	278
7	369	307
9	339	347
11	538	280
Fused silica	168	168

The results from FTIR spectra, TGA and BET surface area measurements show that the decrease of –OH and Si-O-C peaks correlates to an increment of ceramic yield and surface area.

4.4.2 Scanning Electron Microscope (SEM)

The morphology of the hydrolyzed aggregates was observed by scanning electron microscopy, as shown in figure 4.19 (a) and (b). Each shows the characteristic of a dried gel, under acidic and base conditions, respectively. However certain differences in morphology are evident which can be traced to effects of the different catalysis used. Under acid catalysis, the hydroxylated monomer is formed via electrophilic (H^+) reaction. The condensation reaction continues to react via these hydroxylated monomers.

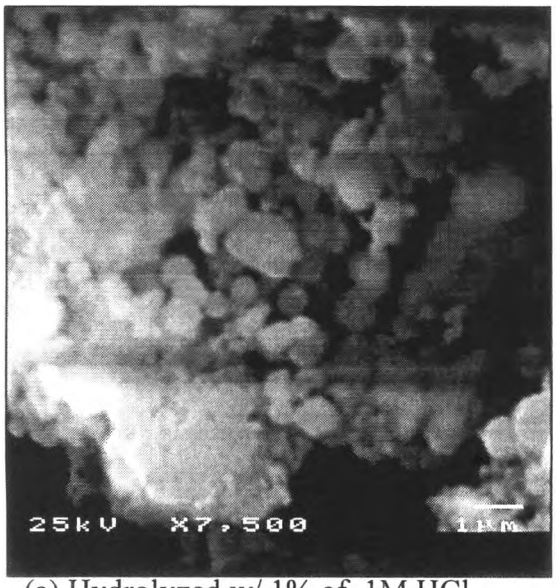

(a) Hydrolyzed w/ 1% of 1M HCl

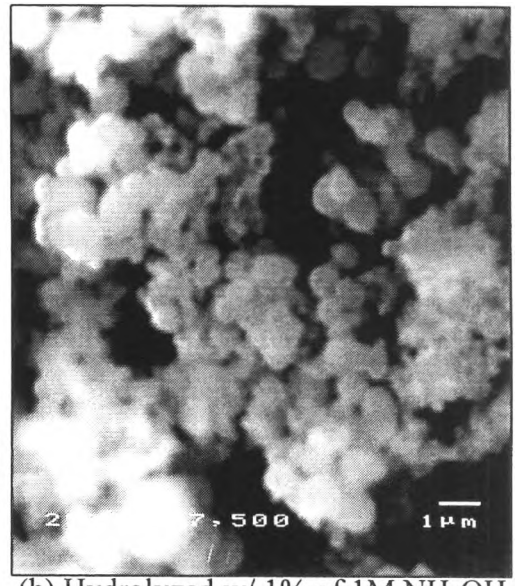

(b) Hydrolyzed w/ 1% of 1M NH_4OH

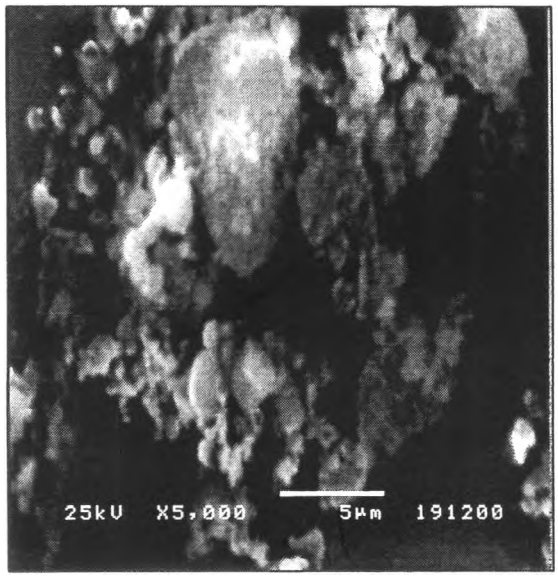

(c) Pyrolysis of material (a) at 750°C, 7 h.

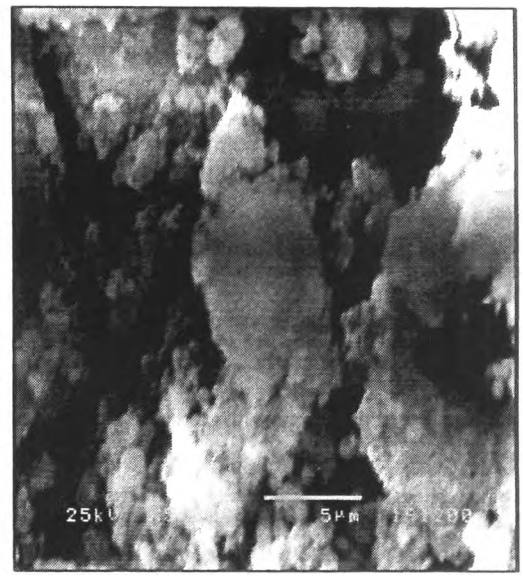

(d) Pyrolysis of material (b) at 750°C, 7 h.

Figure 4.19 SEM of hydrolyzed (a and b) spirosilicate C2 and pyrolyzed (c and d).

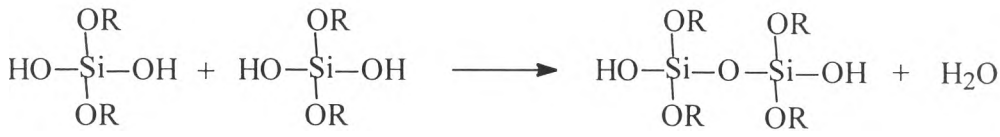

Using base catalysis, (b) the sol particles formed tend to repel each other due to a high surface charge from SiO^- groups, formed according to the following reaction.

$$Si\text{-}OH + OH^- \longrightarrow SiO^- + H_2O$$

Obviously, each conditions has a different influence on the rate of condensation and porosity of the dried gel product.

Effect of Catalysts on Reaction Time: Acid catalyst promote the minimum reaction at 1% of 1M HCl at a pH near the iso-electric point, which gives no electrostatic particle repulsion, (near pH= 2-2.5 (Iler, 1979)). By increasing the concentration of the catalyst, reaction rate increases and the gelling time is reduced. On the other hand, the base-catalyzed reaction takes place via nucleophilic reaction (Yamane, 1988). Since the condensation reaction provides SiO^-, resulting in faster condensation before completely hydrolysis.

Effect of Catalyst on Gel Properties: Using base catalyst, repulsion of the sol structure gave more time for particles to rearrange. Larger particles tend to form first. This is different from using acid catalyst, occurring via addition reaction in which many small molecules tend to grow slowly (LaCourse, 1988). The SEM micrograph in figure 4.19 (b) shows that the porosity of the sol structure is greater than that of (a).

In fact, the gel consists of two phase, the network solid phase and the connected pores filled with liquid phase (Ropp, 1992). As the heat

treatment is applied, the gel shrinks under capillary force as the liquid evaporates. It can be seen in figure 4.19 (a) that the HCl catalyzed gel contains small pores. If it originally contained a large amount of water molecule in the pores, upon heating the gel, the water generated from the concentration of hydroxyl groups leads to a higher shrinkage of the gel, figure 4.19 (c), On the other hand, the ammonia-catalyzed gel contains large pores and small amount of water molecules, smaller shrinkage occurs.

4.5 Density Measurement

The density measurement of product obtained from hydrolyzed gel using 1% HCl of 1M gave a density value less than fused silica, as shown in table 4.12.

Table 4.12 The density measurement of pyrolyzed product: C2 and fused silica (starting material).

Type of products	Density value (g/cm^3) at 25°C
C2	0.54
Fused-silica	2.42

The density of hydrolyzed monomer C2 was lower than fused silica due to the fact that the removal of alkoxy and hydroxyl groups by condensation reaction when the gel was heated, causes a large weight loss, produces new crosslinks and stiffening the structure. In the case of fused silica, a network structure has only small hydroxyl groups on the surfaces thus there is not significant effect on the stiffness of the structure (George, 1989).

4.6 Sol-Gel Transition Study of Poly(Glycolato-Silicate) (Polymer C2)

4.6.1 Fourier Transform Infrared (FTIR) Spectroscopy

The FTIR spectra of polymer hydrolyzed with 1% of 1M HCl and NH_4OH show no difference at room temperature due to the difficulty to hydrolyze crosslinked polymers. Figure 4.20 shows the results for polymer hydrolyzed using 1% of 1M HCl at 40° and 60°C. A decrease in absorption peaks at 3405, 2951, 2883, 1086 and 883 cm^{-1} was observed similar to that produced from C2 monomer.

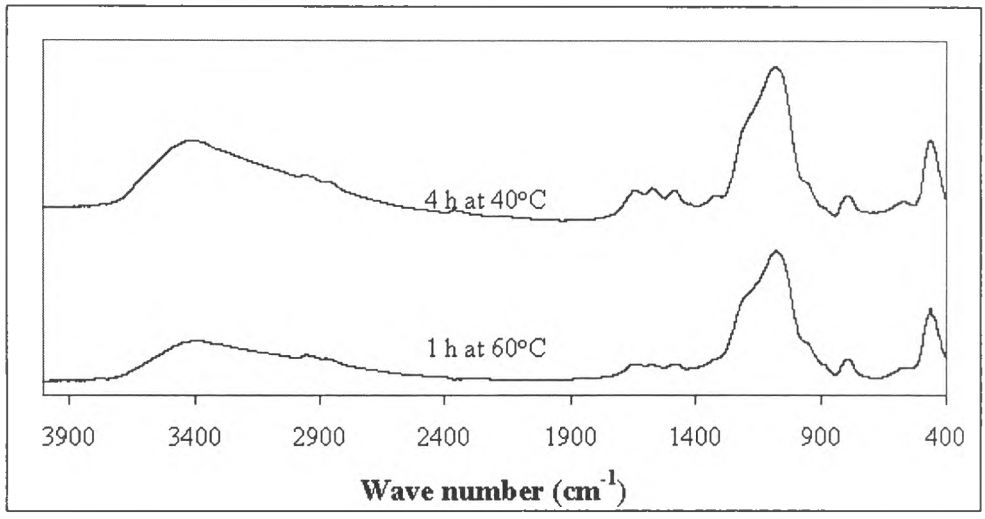

Figure 4.20 FTIR spectra showing the effect of temperature on the hydrolyzed polymer product.

4.6.2 Thermogravimetric Analysis (TGA)

The final ceramic yields of the polymer, as shown in figure 4.21, hydrolyzed at 40° and 60°C were 56.73% and 63.66%, respectively, meaning that a higher ceramic yield was obtained, i.e. more crosslinking of Si-O-Si.

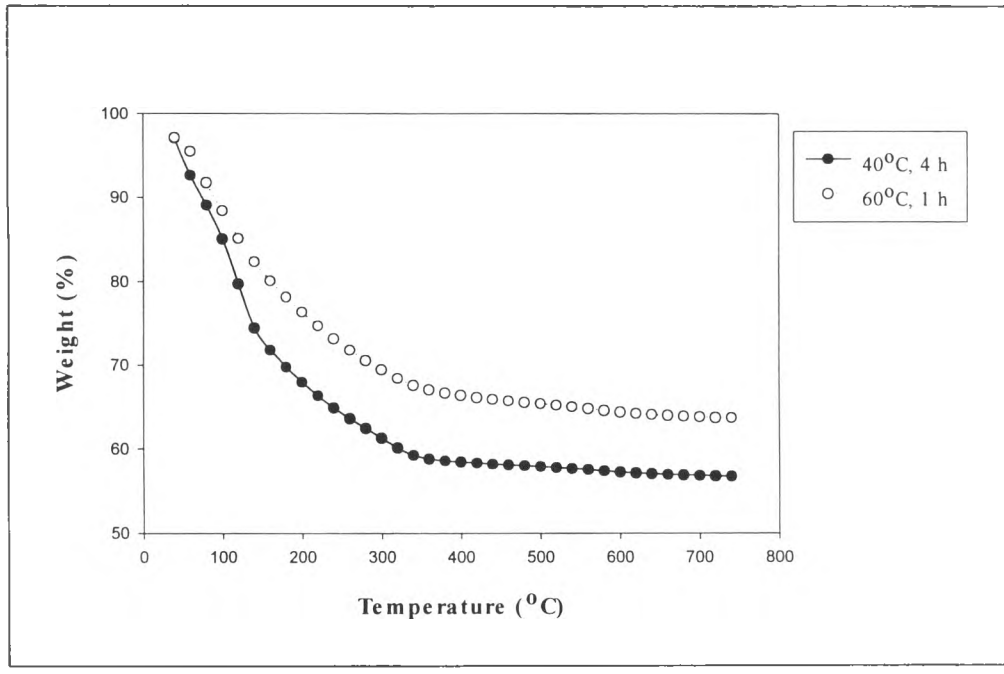

Figure 4.21 TGA thermograms showing percent ceramic yields of hydrolyzed polymer at 40° and 60°C.

4.7 Characterization of Pyrolysis of Poly(Glycolato Siloxane)

4.7.1 BET Surface Area Measurement

The BET surface area analysis of pyrolyzed polymer products at 750°C for 7 h, is shown in table 4.13. As compared to the table 4.11 showing the values of pyrolyzed monomer products, the pyrolyzed polymer products had less surface area than the pyrolyzed monomer products.

Table 4.13 The BET surface area measurement of pyrolyzed C2 polymer and fused-silica.

Type of product	Surface area (m^2/g)
	Multi point BET
1% HCl at RT	231
1%NH_4OH at RT	215
1% HCl at 40°C	180
1% HCl at 60°C	204
Fused-silica	168

4.7.2 Wide angle X-Ray Diffractometer (WXRD)

Figure 4.22 shows the XRD patterns of pyrolyzed monomer and polymer, as compared to fused silica. The resulting diffraction patterns consist of a broad featureless band, showing the non-crystalline amorphous solid form.

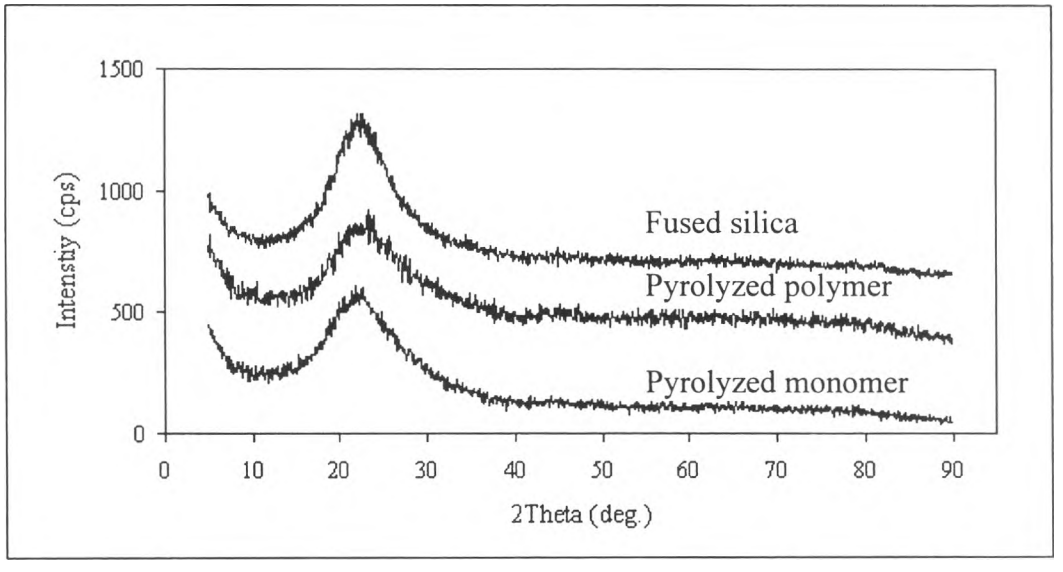

Figure 4.22 XRD patterns of pyrolyzed monomer, pyrolyzed polymer and fused- silica.

4.8 Sol-Gel Transition Study of Aminospirosilicate C4

4.8.1 Fourier Transform Infrared (FTIR) Spectroscopy

C4 Aminospirosilicate is 6-membered ring spirosilicate. The rings are more stable than 5-membered ring C2 spirosilicate. Morover, C4 spirosilicate is bulkier. As the result, C4 hydrolyzed with 1M HCl and NH_4OH showed no differences between room temperature and 40°C. 1M HCl also showed no difference on the hydrolysis even at 60°C. Figure 4.23 thus shows only the results of C4 hydrolyzed using 100% of 1M NH_4OH at 60°C. The decrease in absorption peaks at 3405, 2951, 2883, 1086 cm^{-1} indicate results similar to the structure of silica.

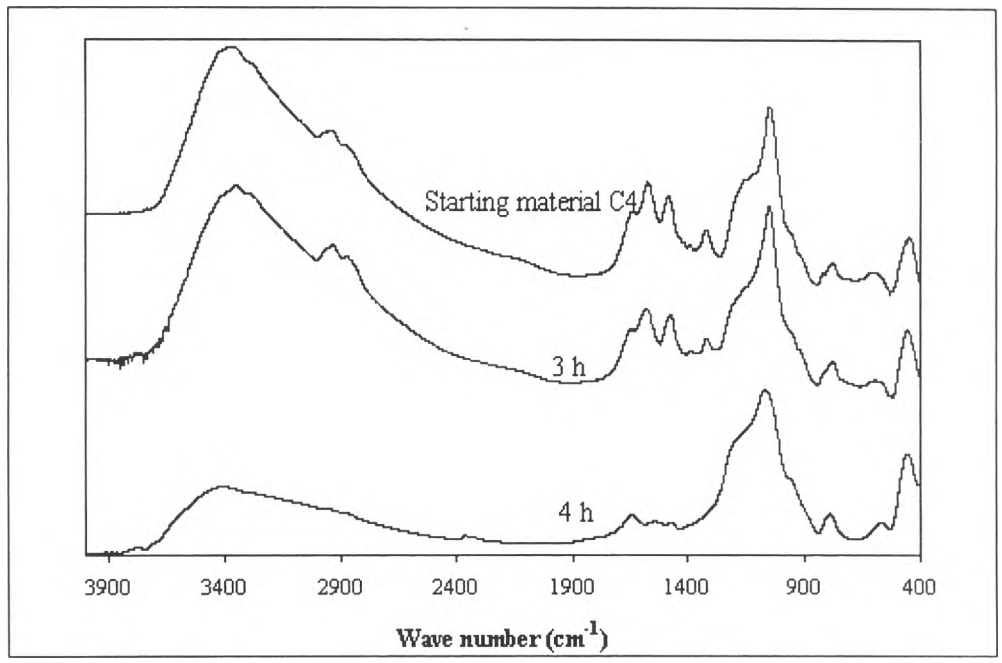

Figure 4.23 FTIR spectra showing the effect time on the hydrolyzed C4 product at 60°C.

4.8.2 Thermogravimetric Analysis (TGA)

The final ceramic yield of the polymer, hydrolyzed at 60°C for 4 h, was 70.89%, as shown in figure 4.24, the higher ceramic yield obtained is due to high concentration of reaction groups under base-catalyzed reaction and high temperature resulting in less time to arrange the molecules to allow crosslinking of Si-O-Si.

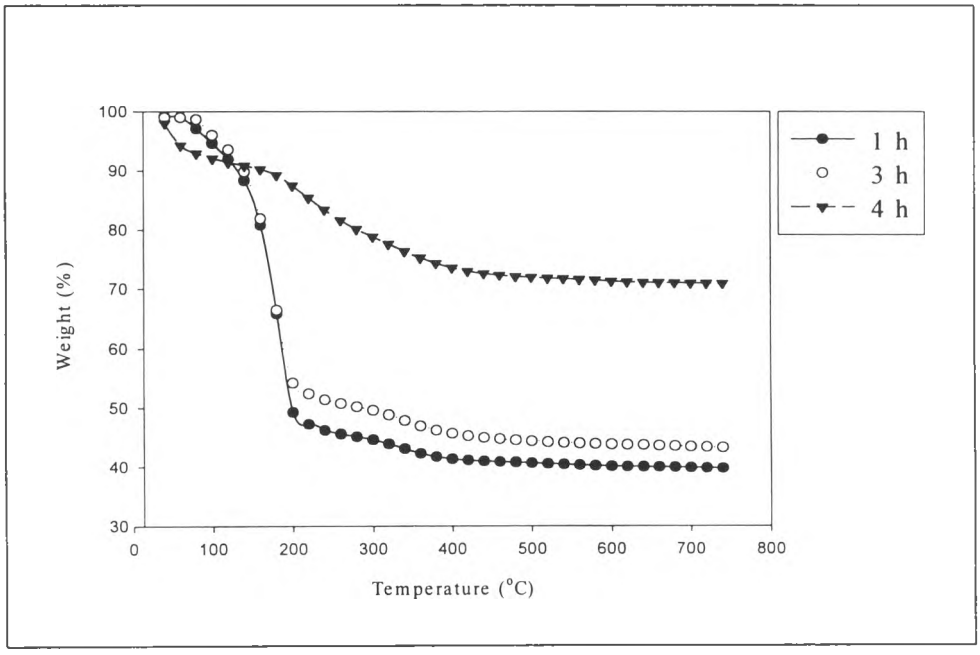

Figure 4.24 TGA thermogram showing percent ceramic yield of hydrolyzed aminospirosilicate, C4 at 60°C for 1, 3 and 4 h.

4.8.3 BET Surface Area Measurement

The BET surface area analysis of aminospirosilicate, C4 pyrolyzed products at 750°C for 7 h was 82.93 m^2/g, reflecting the increase of reaction rate because of the increase in concentration of catalyst and temperature (LaCourse, 1988)

That is, under acidic condition, protonation of alkoxy group is retarded due to the more stable ring structure, more steric hindrance, and the presence of amino group in the structure. It results in no structural change during hydrolysis of the products under acid condition, as shown in figure 4.25

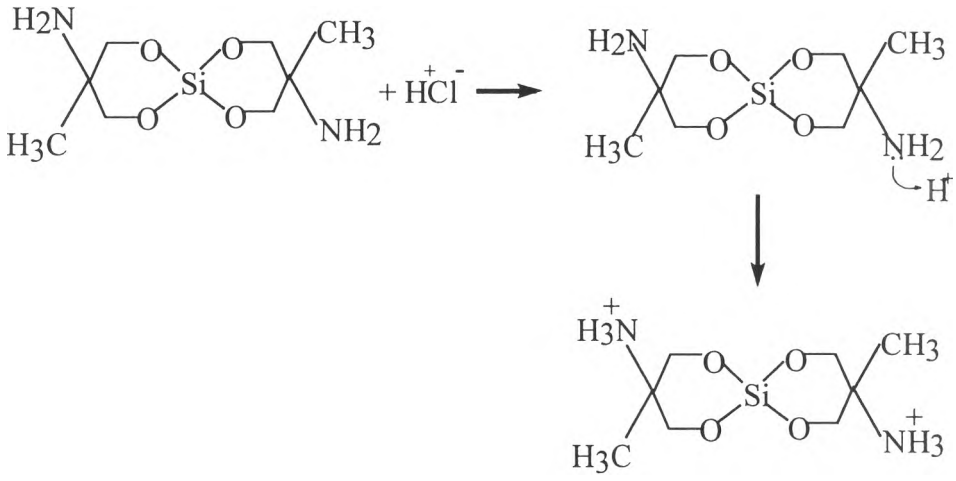

Figure 4.25 The proposed mechanism occurring during hydrolysis of amino-spirosilicate C4 with HCl solution.

4.9 Sol-Gel Transition Study of C4 Polymer

The synthesized products of C4 polymer were extremely difficult to hydrolyze due to the steric hindrance in the structure. Moreover, the opening of the rings caused the molecule to come close together (Varangkana, 2001). The product that was processed and hydrolyzed using both HCl and NH_4OH solution did not exhibit any changes when investigated with spectroscopy technique (FTIR) whether using 2M NH_4OH at 60°C.